catalysts

MDPI

Article

Surface Modification of a MOF-based Catalyst with Lewis Metal Salts for Improved Catalytic Activity in the Fixation of CO_2 into Polymers

Sudakar Padmanaban and Sungho Yoon *

Department of Chemistry, Chung-Ang University, Seoul 156-756, Korea; sudakar.p@outlook.com
* Correspondence: sunghoyoon@cau.ac.kr

Received: 10 September 2019; Accepted: 23 October 2019; Published: 26 October 2019

Abstract: The catalyst zinc glutarate (ZnGA) is widely used in the industry for the alternating copolymerization of CO_2 with epoxides. However, the activity of this heterogeneous catalyst is restricted to the outer surface of its particles. Consequently, in the current study, to increase the number of active surface metal centers, ZnGA was treated with diverse metal salts to form heterogeneous, surface-modified ZnGA-Metal chloride (ZnGA-M) composite catalysts. These catalysts were found to be highly active for the copolymerization of CO_2 and propylene oxide. Among the different metal salts, the catalysts treated with $ZnCl_2$ (ZnGA-Zn) and $FeCl_3$ (ZnGA-Fe) exhibited ~38% and ~25% increased productivities, respectively, compared to untreated ZnGA catalysts. In addition, these surface-modified catalysts are capable of producing high-molecular-weight polymers; thus, this simple and industrially viable surface modification method is beneficial from an environmental and industrial perspective.

Keywords: heterogeneous catalysis; metal organic framework; surface modification; Zinc glutarate; CO_2 fixation; polycarbonate

1. Introduction

In recent decades, anthropogenic activities have dramatically increased the concentration of atmospheric CO_2; this concentration was found to be higher than 400 ppm in 2017 [1]. The rapid increase in the CO_2 content in the atmosphere makes CO_2 a major greenhouse gas. Consequently, the development of efficient and safe methods for capturing and sequestering CO_2 is garnering increased attention. Furthermore, the development of methods and processes for converting CO_2 into value-added chemicals is of paramount interest because CO_2 is a cheap, non-toxic, and abundant carbon feedstock [2,3]. Recently, a great deal of research has been devoted to capturing and utilizing CO_2 to synthesize a variety of value-added products [4–17].

One of the most sustainable strategies for utilizing CO_2 is the copolymerization of CO_2 with epoxides to produce poly(alkylene carbonates). These materials are commercially viable owing to their vast number of applications, such as in adhesives, packing and coating materials, and ceramic binders [18–22]. Furthermore, these polycarbonates are biodegradable and are useful in biomedical applications [19]. The alternating copolymerization of CO_2 with epoxides was first reported by Inoue et al., who used a diethylzinc–water system as a catalyst [23,24]. Subsequently, numerous homogeneous and heterogeneous catalytic systems have been developed. For example, homogeneous catalysts, such as metalloporphyrins, β-diiminate Zn complexes, and metal salen complexes have been found to be highly active for the copolymerization of CO_2 and epoxides [25–27]. Nevertheless, the industrial utilization of these homogeneous catalysts is limited because of their complicated syntheses, the use of toxic metals like chromium, and the difficulties in separating the catalyst/product mixtures.

However, heterogeneous catalysts are preferred for industrial scale applications owing to their low cost, easy synthesis, facile separation from products, and reusability [28–31]. Among the heterogeneous catalysts, zinc dicarboxylates, Zn-Co double metal cyanide complexes, and ternary rare-earth complexes are found to be particularly active for the copolymerization of CO_2 and epoxides. Among them, the zinc glutarate (ZnGA) is widely applied in industry as a catalyst for the copolymerization of propylene oxide (PO) and CO_2 because it is economic, non-toxic, easy to synthesize, and, most beneficially, it yields copolymers with high molecular weights [18,32]. Based on a recent life cycle assessment study, for each one kg of CO_2 incorporated into polycarbonate polyols, up to three kg of CO_2-equivalent greenhouse gas emissions could be reduced [33]. Therefore, improving the productivity of ZnGA becomes necessary in order to meet the increasing economic and environmental requirements.

Despite a growing need and the continued efforts by researchers, the catalytic activity of ZnGA has improved only marginally over the past few decades. Rieger et al. reported on the considerable improvement of the catalytic activity of ZnGA via the introduction of zinc-ethylsulfinate initiator groups to its surface [34]. However, this post-modification has limited industrial viability because of its procedural complexity and use of expensive precursors. Ree et al., demonstrated the effects of different zinc and glutarate sources in the synthesis of ZnGA and consequently the effects of different morphologies of ZnGA on its catalytic activity for CO_2/PO copolymerization [35]. Through continuous research effort, the catalytic activity of ZnGA has been found to be dependent on its surface area and crystallinity [18,36–38]. Recently, the precise structure of ZnGA was obtained by single-crystal X-ray diffraction studies, thus revealing that its catalytic activity mainly originates on the outer surfaces of the Zn-dicarboxylate particles [39]. It should nevertheless be noted that the crystal structure of ZnGA features a 3D-network structure of glutarate ligands and Zn atom of the molecule in which, each Zn atoms tetrahedrally bind to the oxygen atoms of four different glutarate units.

According to the recent definition of metal organic framework (MOF) by Seth and Matzger, ZnGA can be considered a MOF [40]. It is noteworthy that most other Zn-based MOF systems have been reported to yield cyclic carbonate as the predominant product in the reaction of CO_2 and an epoxide, whereas the ZnGA system produces the poly(alkylene carbonate) as the major product [41–47]. In recent years, most studies on ZnGA have focused on increasing its surface area and crystallinity using different supporters, amphiphilic templates, and ultrasonic treatment [48–51]. Furthermore, a recent mechanistic study on CO_2/PO copolymerization using ZnGA indicated a bimetallic mechanism involving sequential insertions of CO_2 and epoxide into Zn-alkoxide and Zn-carboxylate initiator groups on the surface of the catalyst [52]. The optimal separation between two adjacent Zn atoms was suggested to be in the range 4.3–5.0 Å, which results in the optimal activation energy required for copolymerization. Recently, we explored the catalytic ability of ZnGA for the copolymerization of CO_2 with a relatively reluctant epoxide, epichlorohydrin, and the application of ZnGA as a catalyst for the terpolymerization of CO_2, PO, and β-butyrolactone [53,54].

As a part of our continued research effort to develop heterogeneous catalysts for CO_2 conversions, this study reports a facile method for preparing a surface modified ZnGA and its enhanced catalytic activity in the CO_2/PO polymerization. In order to improve the catalytic activity of ZnGA, the number of active sites on the surfaces of the catalyst particles must be increased. It has been reported that ZnGA has protruding glutarate and hydroxyl groups on its surface that act as initiators for CO_2/PO copolymerization [55,56]. These glutarate and hydroxyl groups can ligate additional incoming metal ions and create oxygen-bound metal centers on the surface of the ZnGA. Therefore, we hypothesized that surface modification of ZnGA by treatment with Lewis metal ions to form metal-treated ZnGA catalysts (ZnGA-M) would increase the number of active metal centers on the surface of the ZnGA, as depicted in Figure 1. This would provide catalysts with improved cooperative bimetallic properties for CO_2/PO copolymerization (Scheme 1). Indeed, the pore structure of some MOFs were modified by the installation of additional ligand motif to coordinate additional metal centers in a step called "post synthetic modification" (PSM) [57–61]. However, in the case of ZnGA frameworks, the protruding glutarate groups may be considered for this purpose. To test this hypothesis, different metal chlorides,

i.e., $FeCl_3$, $AlCl_3$, $ZnCl_2$, and $CoCl_2$, were selected for the preparation of ZnGA-M catalysts based on their activities in homogeneous complexes species. The resulting catalysts were subsequently assessed for their activities in CO_2/PO copolymerization.

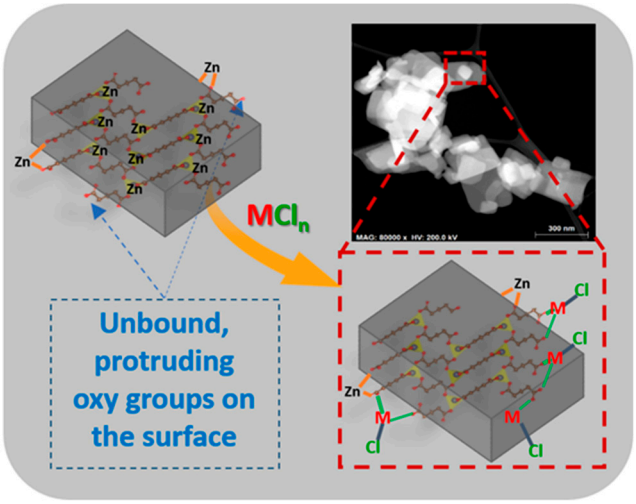

Figure 1. Schematic representation of the formation of ZnGA-M.

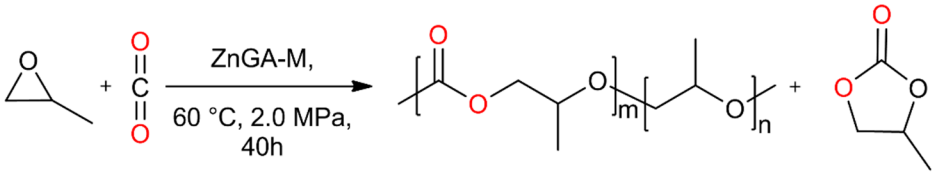

Scheme 1. Copolymerization of CO_2 and PO using ZnGA-M.

2. Results and Discussion

2.1. Synthesis and Characterization of Catalysts

Initially, standard ZnGA (std-ZnGA) was prepared according to a published procedure with slight modifications [62]. Figure S1 compares the powder X-ray diffraction (PXRD) pattern of the resultant white precipitate with the pattern calculated from the crystal structure and confirms the formation of std-ZnGA in its pure form with relatively high crystallinity (Figure S1). Fourier-transform infrared (FT-IR) spectroscopic analysis shows typical peaks for ZnGA. The CH_2 scissoring and CH stretching bands were observed at 1445 cm^{-1} and 2955 cm^{-1}. The bands at ~1585 cm^{-1} and ~1405 cm^{-1} correspond to COO^- antisymmetric stretching frequencies. The COO^- symmetric stretching band was observed at 1538 cm^{-1} (Figure S2a). Figure S3a shows a scanning electron microscopy (SEM) image in which the std-ZnGA has taken the form of typical platelet-shaped particles. These analyses collectively confirm the formation of std-ZnGA according to the previous reports in the literature.

The ZnGA-M catalysts were then prepared in anhydrous THF through treatment with different metal chloride solutions at different ratios, as shown in Table 1. The copolymerization of CO_2 and PO requires sequential insertion of CO_2 and PO into the Zn-alkoxide and Zn-carboxylate initiator groups on the surface of the catalyst. Therefore, the metal treatment should be kept as mild as possible to effect synchronized cooperative catalysis because a thick coating of metal chloride would block the monomers from approaching the catalytic sites. Thus, the ratio of metal to Zn was maintained in the range of 10^{-3}–10^{-4} equivalents in the metal treatment step.

The metal-treated ZnGAs were analyzed via PXRD, FT-IR spectroscopy, and SEM and TEM analyses. The FT-IR spectra of the ZnGA-M catalysts are shown in Figure S2a. The FT-IR analysis shows that the metal treatment does not affect the original glutarate binding, since the amount of each metal salt used is too small. As shown in Figure S2b, the amounts of metal ions used are too

low to cause any phase changes in the crystal lattice or structural deformations. Thus, the PXRD patterns of all the catalysts are similar. Figure S3 shows the SEM images of the ZnGA-M samples and reveals that the metal treatments do not significantly change the morphology. The metal ions cannot be detected via SEM energy-dispersive X-ray spectroscopy (SEM-EDS) analysis when fewer than 10^{-2} equivalents of the metal ions are used. However, the scanning transmission electron microscopy (STEM) and energy-dispersive X-ray spectroscopy (EDS)-assisted elemental mapping of Al and Zn in ZnGA-Al-10^{-3} reveal the homogeneous distribution of Zn and Al metals in the ZnGA-Al-10^{-3} (Figure 2). In addition, the actual coated amount of Al in ZnGA-Al-10^{-3} was obtained via inductively coupled plasma optical emission spectroscopy (ICPOES), in which the ratio of Zn to Al was found to be 1:1.1 × 10^{-3}. Similarly, the ratio between Zn and Fe in ZnGA-Fe-10^{-3} was found to be 1:1.0 × 10^{-3}. These analyses confirmed the attachment of the different metal ions after metal treatment.

Table 1. Copolymerization of CO_2 with PO using ZnGA-M catalysts [a].

Entry	Catalyst	Zn:MCl_n [b]	TON [c]	Productivity Increment [d] (%)	Fco_2 [e]	Selectivity (%) [f]		M_n [g] (kg/mol)	PDI [g]	T_g [h] (°C)
						PPC	PC			
1	Std-ZnGA	1:0	72.4	-	94.9	96.0	4.0	156.4	3.5	42
2	ZnGA-Fe-10^{-3}	1:10^{-3}	82.5	13.9	94.8	98.0	2.0	137.6	2.8	38
3	ZnGA-Fe-10^{-4}	1:10^{-4}	90.9	25.6	94.1	94.0	6.0	262.4	2.0	40
4	ZnGA-Al-10^{-3}	1:10^{-3}	88.7	22.5	93.5	96.0	4.0	196.3	1.8	36
5	ZnGA-Al-10^{-4}	1:10^{-4}	77.5	1.5	95.1	98.0	2.0	231.8	2.2	35
6	ZnGA-Zn-10^{-2}	1:10^{-2}	72.0	−0.5	93.7	98.0	2.0	99.8	3.9	42
7	ZnGA-Zn-10^{-3}	1:10^{-3}	100.1	38.3	94.9	97.0	3.0	208.0	1.8	38
8	ZnGA-Zn-10^{-4}	1:10^{-4}	80.7	11.5	91.7	96.0	4.0	147.8	2.2	37
9	ZnGA-Co-10^{-3}	1:10^{-3}	72.0	−0.5	92.2	95.0	5.0	144.4	1.9	34
10	ZnGA-Co-10^{-4}	1:10^{-4}	73.6	1.7	93.5	95.0	5.0	70.7	2.4	35
11	ZnGA-Al-1	1:1	8.1	-	36.2	91.0	9.0	-	-	-

[a] Conditions: 0.20 g catalyst; 20.0 mL PO; 2.0 MPa CO_2; 60 °C and 40 h. [b] Treated mol ratio of ZnGA and metal salt. [c] TON = weight of polymer formed per gram of catalyst. [d] Values represent the increment in productivity of the metal-treated catalysts in comparison to std-ZnGA. [e] Fco_2 of the polymers was determined from ^{1}H NMR spectra of the polymers. [f] Obtained from ^{1}H NMR spectra of the polymers; PC = propylene carbonate. [g] M_n, M_w, and PDI values of the polymers were determined using GPC with polystyrene standards in THF. [h] Determined from DSC.

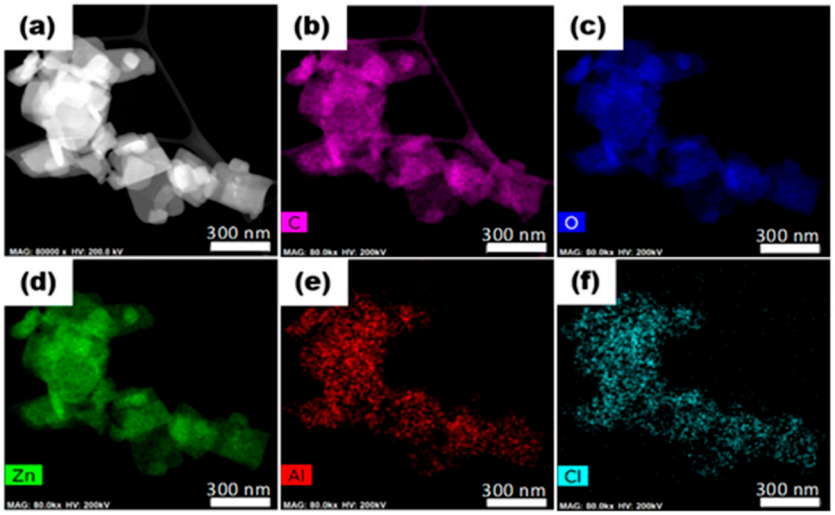

Figure 2. STEM image and EDS mapping. (**a**) STEM image of ZnGA-Al-10^{-3}; STEM-EDS mapping of (**b**) C (purple), (**c**) O (blue), (**d**) Zn (green), (**e**) Al (red), and (**f**) Cl (cyan) elements in ZnGA-Al-10^{-3}; (Scale bar: = 300 nm).

2.2. Catalytic Activity Studies

To see the effect of metal treatment in the copolymerization of CO_2 and PO, the catalytic activities of the metal-treated ZnGAs were assessed and compared with those of std-ZnGA. All the copolymerization reactions were performed using 0.20 g of catalyst and 20.0 mL PO under 2.0 MPa CO_2 at 60 °C for 40 h. The results are summarized in Table 1. The productivity or the turnover number (TON) is given as grams of PPC formed per gram of catalyst (g PPC/g catalyst). The carbonate content (Fco_2) values of the poly(propylene carbonate)-co-polyethers produced were determined using ^{1}H NMR spectroscopy according to the following equation:

$$Fco_2 = [(A_{5.0} + A_{4.2})/(A_{5.0} + A_{4.2} + A_{3.8–3.5})] \times 100 \quad (1)$$

where A represents the integral area of the corresponding protons in the ^{1}H NMR spectrum.

In an initial trial, the std-ZnGA produced poly(propylene carbonate) (PPC) with 93.9% Fco_2 and a turnover number (TON) of 72.4 g of PPC/g of catalyst. The resultant polymer has a molecular weight of 156.4 kg/mol and a polydispersity index (PDI) of 3.5 (entry 1, Table 1). Then the ZnGA-M catalysts were used as catalysts for the copolymerization of CO_2 and PPO. The results are summarized in Table 1. From Table 1, it is evident that the metal-treated catalysts show a significant increment in TON for CO_2/PO copolymerization, and the activity increments are in the range of 1.6–38.3%. Among the metal-treated ZnGA catalysts, ZnGA-Al, ZnGA-Fe, and ZnGA-Zn show dramatic improvements in productivity compared to that of std-ZnGA, with TONs ranging from 80.7 to 100.1 (entry 2–5, 7, and 8, Table 1). It is noteworthy that treatment with 10^{-3} equivalents of $ZnCl_2$ results in a TON of 100.1, which is ~38% higher than that of std-ZnGA (entry 7, Table 1).

For $AlCl_3$ and $ZnCl_2$, the catalytic activities increase following a rise in the amount of metal from 10^{-4} equivalents to 10^{-3} equivalents (entry 4, 5, 7, and 8, Table 1). Conversely, $FeCl_3$ shows a slight decline in the TON after an increase in the metal treatment amount from 10^{-4} equivalents to 10^{-3} equivalents (entry 2 and 3, Table 1). In addition, when increasing the $ZnCl_2$ amount to 10^{-2} equivalents, the observed productivity is lower than that of std-ZnGA (entry 6, Table 1). These results suggest that there is a threshold limit for the amount of metal ions employed, beyond which the metal ions cover the whole surface of the ZnGA and block the monomers from approaching the active Zn-metal bimetallic sites. This masking effect is repeated when using $CoCl_2$ as the metal salt, because Co^{2+} ions are inactive when used in homogeneous salen complexes and they need to be oxidized to Co^{3+} for higher catalytic performance [63]. Importantly, increasing the amount of $CoCl_2$ has a negative effect on copolymerization, and the productivity of ZnGA-Co-10^{-3} is decreased by ~0.5% (TON = 72.0).

As an extreme example, std-ZnGA was treated with 1.0 equivalent of $AlCl_3$ for 24 h and the resultant white particles were probed using SEM analysis. The SEM image shows that the surface of the ZnGA is completely covered with a thick layer of $AlCl_3$, with the $AlCl_3$ also having round-shaped edges (Figure 3). TEM-EDS mapping had shown the homogeneous distribution of Zn and Al atoms throughout the sample (Figure S4). The ratio of Zn to Al as shown by TEM-EDS is 1 to 7.4, suggesting a thick layer of Al-motif covered the surface. Additionally, the FT-IR spectrum of ZnGA-Al-1 shows a broad hydroxyl stretching in the range of 3000–3500 cm^{-1}. This is different from other ZnGA-M samples (Figure S5). Therefore, as shown in Figure S6, when increasing the amount of metal salt beyond a specific limit, the excess metal salt form a thick layer resembling the bulk metal chloride, thus rendering the catalyst less active (entry 11, Table 1). This fact accounts for the reduced activity of ZnGA-Zn-10^{-2} (entry 6, Table 1). These results clearly show that the presence of other metal ions influences the reactivity of the Zn atoms on the surface of the ZnGA catalyst. Additionally, the added metal on the surface may create a Zn-O-M bimetallic site with optimal distance between the surface metal centers. As reported for a number of homogeneous di-nuclear or bimetallic catalysts, the reaction pathway may follow a bimetallic-cooperative mechanism, wherein one metal may selectively bind with epoxide and ease the ring opening, while the other metal activates the CO_2 and attacks the activated

epoxide to form the metal carbonate bond [52]. Alternate additions of epoxide and CO_2 results in a polymer chain growth.

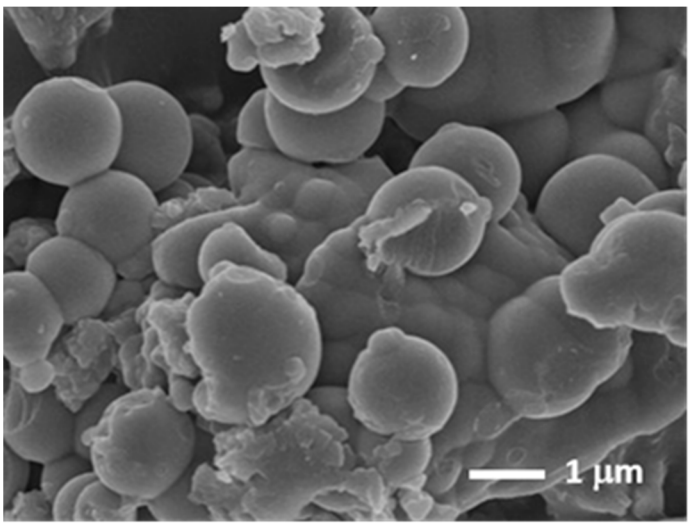

Figure 3. SEM image of ZnGA-Al-1 showing thick layers of $AlCl_3$ on the ZnGA.

2.3. Properties of Polymers

The polymers formed using the different ZnGA-M samples were then characterized with ^{1}H NMR spectroscopy, differential scanning calorimetry (DSC), thermogravimetric analysis (TGA), and Gel Permeation Chromatography (GPC). The ^{1}H NMR spectrum of the polymer exhibits the methyl, methylene, and methine peaks of the polycarbonate at 1.3 ppm, 4.2 ppm, and 5.1–4.9 ppm, respectively (Figure S7).

It is worth mentioning that all these catalysts produce copolymers with significantly high TONs at a relatively low CO_2 pressure of 2.0 MPa, while the Fco_2 values are in the range 90–95% with a very small amount of polyether linkages. The microstructure of the polymers was analyzed by ^{13}C NMR analysis. This revealed that the polymers are formed with a predominantly head-to-tail (HT) connectivity (Figure S8). The molecular weight distributions of the prepared polycarbonates were then analyzed using GPC with polystyrene standards in THF and the GPC elugrams. Some of the selected polymers are shown in Figure S9. The results demonstrate that the cooperative bimetallic catalysts actually help to produce polymers with very high molecular weights. As seen in the Table 1, all the catalysts except ZnGA-Co-10^{-4} and ZnGA-Zn-10^{-2} produce polymers with high M_n values and PDI values close to 2.0. Interestingly, ZnGA-Fe-10^{-4} affords a polymer with the very high M_n of 262.4 kg/mol. The PDIs of the polymers varied from 1.8 to 3.5.

The TGA results of the polycarbonates show that the 5% weight loss temperatures ($T_{5\%}$) of the polymers are around 230 °C and complete decomposition occurs in the range 330–350 °C. However, the glass transition temperatures (T_g) of the resulting polymers are slightly lower than that of the polycarbonate produced using std-ZnGA and vary from 33–38 °C (Figure S10). These values are in the accepted range typically reported for PPC prepared from ZnGA under different conditions.

3. Experimental Section

3.1. Materials and Methods

Glutaric acid (≥99.0%) was obtained from Tokyo Chemical Industry Co., Ltd. and used without further purification. Anhydrous $ZnCl_2$, ZnO, $FeCl_3$, $CoCl_2$, $AlCl_3$, and anhydrous tetrahydrofuran (≥99.9%) were purchased from Sigma-Aldrich (Seoul, South Korea) and used as received. Propylene oxide (≥99.9%, PO) was received from Sigma-Aldrich and was distilled over CaH_2 before use. CO_2 gas (99.999) was received from Shinyang gas Industries, Korea. Powder X-ray diffraction

(PXRD) measurements were performed using a Bruker D8 Focus X-ray powder diffractometer (Billerica, MA, USA) using CuKα radiation at room temperature. A Hitachi (Tokyo, Japan.) FE-SEM S-4800 and TEM-Talos; F 200X system were used to study the morphologies of the catalysts. The Fourier-transform-infrared (FT-IR) spectra were measured on Nicolet iS 50 (Thermo Fisher Scientific, Waltham, MA, USA) spectrometer. Metal contents in the catalysts were analyzed using inductively coupled plasma optical emission spectroscopy (ICP-OES) (iCAP-Q, Thermo Fisher Scientific, Waltham, MA, USA) and a microwave-assisted acid digestion system (MARS6, CEM/U.S.A). Bruker Ascend 400 MHz spectrometer was used for measuring the ^{1}H and ^{13}C NMR spectra of the products. Gel Permeation Chromatography (GPC) analysis was performed using a Waters 717 plus instrument equipped with a Waters 515 HPLC Pump (Milford, MA, USA). The columns were eluted with THF at a flow rate of 1.00 mL/min at 35 °C. GPC curves were calibrated using polystyrene standard with molecular weight ranges from 580 to 660,500. A 2960 Simultaneous DSC-TGA instrument (TA instruments, New Castle, DE, USA) was used for the Thermogravimetric Analysis (TGA) with a heating rate of 10 °C/min from 25 °C to 500 °C under Nitrogen atmosphere. A PerkinElmer DSC 4000 instrument (Waltham, MA, USA) was used to perform the Differential Scanning Calorimetric (DSC) tests with a heating rate of 10 °C/min from 20 °C to 120 °C under Nitrogen atmosphere.

3.2. Synthesis of std-ZnGA

std-ZnGA was synthesized by following a published report with slight modification [62]. ZnO (100.0 mmol) was suspended in toluene (150 mL) in a 250-mL round-bottom flask equipped with a Dean-Stark trap and a reflux condenser. Glutaric acid (98.0 mmol) was added to this mixture and refluxed at 60 °C with vigorous stirring for 4 h. After 4 h, heating was stopped and the reaction mixture cooled to room temperature. The white precipitate was filtered and washed with excess of acetone. The resulting product was dried under vacuum at 130 °C, delivering 19.00 g of ZnGA (99.2%). The elemental analysis result, calculated (observed) for $C_5H_6O_4Zn$ (%) was C, 30.72(29.89); H, 3.09(3.05); O, 32.74(33.10).

3.3. General Procedure for Preparing Metal Treated Catalysts

3.3.1. Preparation of Metal Chloride Stock Solutions

The metal chloride stock solutions were prepared by dissolving about 40 to 50 μmol of the corresponding metal chloride in anhydrous THF under argon atmosphere.

3.3.2. Metal Treatment of std-ZnGA

To a dispersion of std-ZnGA (0.5 g, 2.55 mmol) in 20.0 mL of anhydrous THF was added a desired amount of the selected metal chloride as a solution in THF under Ar atm. The white suspension was stirred at ambient temperature for 30 min. After that, the white solid was separated by filtration followed by washing with THF (30.0 mL × 2) and acetone (30.0 mL × 2). The resulting solid was dried under vacuum at 60 °C for 10 h.

3.4. General Procedure for the Copolymerization of CO_2 and PO

All copolymerization reactions were carried out in a pre-dried 100 mL stainless steel autoclave reactor equipped with a magnetic stirrer and a programmable temperature controller. In a typical reaction, 20.0 mL of PO was added to 200.0 mg of the desired catalyst under Ar atmosphere and then pressurized with CO_2 to 2.0 MPa at room temperature. The mixture was stirred at 60 °C for 40 h. After cooling the reactor to room temperature, CO_2 was slowly released. A small fraction was taken for ^{1}H NMR analysis and the remaining mass was dissolved in dichloromethane (DCM) and treated with 1.25 M methanolic HCl solution (1.0 mL × 3). The addition of excess methanol to the solution afforded the polymer as a white precipitate and was dried under vacuum at 60 °C.

4. Conclusions

In this study, surface-modified ZnGA samples were prepared by treatment with different metal chloride salts and used as new, highly active catalysts in the copolymerization of CO_2 and PO under a relatively low CO_2 pressure of 2.0 MPa. Among the various metal-treated ZnGA catalysts, ZnGA-Zn-10^{-3} was found to be highly active with a TON of 100.1 g PPC/g catalyst, which is 38.3% higher than that of std-ZnGA (TON = 72.4). The $FeCl_{3-}$ treated catalyst ZnGA-Fe-10^{-4} produced the polymer with the highest molecular weight (262 kg/mol) with a TON of 90.9. These results indicate that this simple and industrially viable procedure effectively increases the catalytic activity of ZnGA. This economically beneficial method promotes the use of the ZnGA-M catalytic system for the industrial applications in the production of biodegradable thermoplastics from PO and CO_2.

Supplementary Materials: The following are available online at http://www.mdpi.com/2073-4344/9/11/892/s1, Figure S1: PXRD pattern of std-ZnGA and PXRD pattern calculated from the crystal structure of ZnGA via Mercury 3.7, Figure S2: (a) FT-IR spectra of std-ZnGA and ZnGA-M catalysts, (b) PXRD patterns of std-ZnGA and ZnGA-M catalysts, Figure S3: SEM images of std-ZnGA and ZnGA-MCl_n, Figure S4: STEM image and EDS mapping. (a) STEM image of ZnGA-Al-1; STEM-EDS mapping of (b) Zn (red)and (c) Al (green) elements in ZnGA-Al-1; (Scale bar: = 200 nm), Figure S5: FT-IR spectra of std-ZnGA and ZnGA-Al-1, Figure S6: Expected coordination modes of MCl_n on the std-ZnGA surface, Figure S7: ^{1}H NMR spectrum of PPC from entry 3 in Table 1, Figure S8: ^{13}C NMR spectrum of PPC from entry 3 in Table 1, Figure S9: GPC elugrams for some selected polymers from Table 1, Figure S10: DSC curves of selected polymers from Table 1.

Author Contributions: S.Y. and S.P. have designed the experiments. S.P. conducted the experiments. S.P. and S.Y. wrote the manuscript and S.Y. supervised the project. All authors reviewed the manuscript.

Funding: This research was supported by a Korea CCS R&D Center (KCRC) grant funded by the Korea government (Ministry of Science, ICT & Future Planning) (No. 2014M1A8A1049300).

Acknowledgments: We acknowledge the financial support provided by the Korea CCS R&D Center (KCRC) grant funded by the Korea government (Ministry of Science, ICT & Future Planning) (no. 2014M1A8A1049300).

Conflicts of Interest: The authors declare that the research was conducted in the absence of any commercial or financial relationships that could be construed as a potential conflict of interest.

References

1. The Keeling Curve. Scripps Institution of Oceanography at University of California at San Diego. Available online: https://scripps.ucsd.edu/programs/keelingcurve/ (accessed on 13 September 2017).
2. Scott, D.A.; Christopher, M.B.; Geoffrey, W.C. Carbon Dioxide as a Renewable C1 Feedstock: Synthesis and Characterization of Polycarbonates from the Alternating Copolymerization of Epoxides and CO_2. In *Feedstocks for the Future*; American Chemical Society: Washington, DC, USA, 2006; Volume 921, pp. 116–129.
3. Aresta, M.; Dibenedetto, A. Utilisation of CO_2 as a chemical feedstock: Opportunities and challenges. *Dalton Trans.* **2007**, *28*, 2975–2992. [CrossRef] [PubMed]
4. Song, C. Global challenges and strategies for control, conversion and utilization of CO_2 for sustainable development involving energy, catalysis, adsorption and chemical processing. *Catal. Today* **2006**, *115*, 2–32. [CrossRef]
5. Spinner, N.S.; Vega, J.A.; Mustain, W.E. Recent progress in the electrochemical conversion and utilization of CO_2. *Catal. Sci. Technol.* **2012**, *2*, 19–28. [CrossRef]
6. Kumar, S.; Verma, S.; Shawat, E.; Nessim, G.D.; Jain, S.L. Amino-functionalized carbon nanofibres as an efficient metal free catalyst for the synthesis of quinazoline-2,4(1H,3H)-diones from CO_2 and 2-aminobenzonitriles. *RSC Adv.* **2015**, *5*, 24670–24674. [CrossRef]
7. Park, K.; Gunasekar, G.H.; Prakash, N.; Jung, K.-D.; Yoon, S. A Highly Efficient Heterogenized Iridium Complex for the Catalytic Hydrogenation of Carbon Dioxide to Formate. *ChemSusChem* **2015**, *8*, 3410–3413. [CrossRef]
8. Gunasekar, G.H.; Park, K.; Jung, K.-D.; Yoon, S. Recent developments in the catalytic hydrogenation of CO_2 to formic acid/formate using heterogeneous catalysts. *Inorg. Chem. Front.* **2016**, *3*, 882–895. [CrossRef]
9. Kim, S.-H.; Chung, G.-Y.; Kim, S.-H.; Vinothkumar, G.; Yoon, S.-H.; Jung, K.-D. Electrochemical NADH regeneration and electroenzymatic CO_2 reduction on Cu nanorods/glassy carbon electrode prepared by cyclic deposition. *Electrochim. Acta* **2016**, *210*, 837–845. [CrossRef]

10. Gunasekar, G.H.; Park, K.; Ganesan, V.; Lee, K.; Kim, N.-K.; Jung, K.-D.; Yoon, S. A Covalent Triazine Framework, Functionalized with Ir/N-Heterocyclic Carbene Sites, for the Efficient Hydrogenation of CO_2 to Formate. *Chem. Mater.* **2017**, *29*, 6740–6748. [CrossRef]
11. Park, K.; Lee, K.; Kim, H.; Ganesan, V.; Cho, K.; Jeong, S.K.; Yoon, S. Preparation of covalent triazine frameworks with imidazolium cations embedded in basic sites and their application for CO_2 capture. *J. Mater. Chem. A* **2017**, *5*, 8576–8582. [CrossRef]
12. Gunasekar, G.H.; Park, K.; Jeong, H.; Jung, K.D.; Park, K.; Yoon, S. Molecular Rh(III) and Ir(III) Catalysts Immobilized on Bipyridine-Based Covalent Triazine Frameworks for the Hydrogenation of CO_2 to Formate. *Catalysts* **2018**, *8*, 295. [CrossRef]
13. Gunasekar, G.H.; Shin, J.; Jung, K.-D.; Park, K.; Yoon, S. Design Strategy toward Recyclable and Highly Efficient Heterogeneous Catalysts for the Hydrogenation of CO_2 to Formate. *ACS Catal.* **2018**, *8*, 4346–4353. [CrossRef]
14. Abbas, I.; Kim, H.; Shin, C.-H.; Yoon, S.; Jung, K.-D. Differences in bifunctionality of ZnO and ZrO_2 in $Cu/ZnO/ZrO_2/Al_2O_3$ catalysts in hydrogenation of carbon oxides for methanol synthesis. *Appl. Catal. B Environ.* **2019**, *258*, 117971. [CrossRef]
15. Gunasekar, G.H.; Jung, K.-D.; Yoon, S. Hydrogenation of CO_2 to Formate using a Simple, Recyclable, and Efficient Heterogeneous Catalyst. *Inorg. Chem.* **2019**, *58*, 3717–3723. [CrossRef] [PubMed]
16. Gunasekar, G.H.; Yoon, S. A phenanthroline-based porous organic polymer for the iridium-catalyzed hydrogenation of carbon dioxide to formate. *J. Mater. Chem. A* **2019**, *7*, 14019–14026. [CrossRef]
17. Kim, C.; Choe, Y.-K.; Won, D.H.; Lee, U.; Oh, H.-S.; Lee, D.K.; Choi, C.H.; Yoon, S.; Kim, W.; Hwang, Y.J.; et al. Turning Harmful Deposition of Metal Impurities into Activation of Nitrogen-Doped Carbon Catalyst toward Durable Electrochemical CO_2 Reduction. *ACS Energy Lett.* **2019**, *4*, 2343–2350. [CrossRef]
18. Luinstra, G.A. Poly(propylene carbonate), old copolymers of propylene oxide and carbon dioxide with new interests: Catalysis and material properties. *Polym. Rev.* **2008**, *48*, 192–219. [CrossRef]
19. Scharfenberg, M.; Hilf, J.; Frey, H. Functional Polycarbonates from Carbon Dioxide and Tailored Epoxide Monomers: Degradable Materials and Their Application Potential. *Adv. Funct. Mater.* **2018**, *28*, 1704302. [CrossRef]
20. Luinstra, G.A.; Borchardt, E. Material Properties of Poly(Propylene Carbonates). *Adv. Polym. Sci.* **2012**, *245*, 29–48. [CrossRef]
21. Alessandra, Q.E.; Gabriele, C.; Jean-Luc, D.; Siglinda, P. Carbon Dioxide Recycling: Emerging Large-Scale Technologies with Industrial Potential. *ChemSusChem* **2011**, *4*, 1194–1215.
22. Peters, M.; Koehler, B.; Kuckshinrichs, W.; Leitner, W.; Markewitz, P.; Müller, T.E. Chemical Technologies for Exploiting and Recycling Carbon Dioxide into the Value Chain. *ChemSusChem* **2011**, *4*, 1216–1240. [CrossRef]
23. Inoue, S.; Koinuma, H.; Tsuruta, T. Copolymerization of Carbon Dioxide and Epoxide. *J. Polym. Sci. Pol. Lett.* **1969**, *7*, 287–292. [CrossRef]
24. Inoue, S.; Koinuma, H.; Tsuruta, T. Copolymerization of Carbon Dioxide and Epoxide with Organometallic Compounds. *Makromol. Chem.* **1969**, *130*, 210–220. [CrossRef]
25. Darensbourg, D.J. Making plastics from carbon dioxide: Salen metal complexes as catalysts for the production of polycarbonates from epoxides and CO_2. *Chem. Rev.* **2007**, *107*, 2388–2410. [CrossRef] [PubMed]
26. Ang, R.R.; Sin, L.T.; Bee, S.T.; Tee, T.T.; Kadhum, A.A.H.; Rahmat, A.R.; Wasmi, B.A. A review of copolymerization of green house gas carbon dioxide and oxiranes to produce polycarbonate. *J. Clean. Prod.* **2015**, *102*, 1–17. [CrossRef]
27. Trott, G.; Saini, P.K.; Williams, C.K. Catalysts for CO_2/epoxide ring-opening copolymerization. *Philos. Trans. R. Soc. A* **2016**, *374*, 20150085. [CrossRef]
28. Sudakar, P.; Gunasekar, G.H.; Baek, I.H.; Yoon, S. Recyclable and efficient heterogenized Rh and Ir catalysts for the transfer hydrogenation of carbonyl compounds in aqueous medium. *Green Chem.* **2016**, *18*, 6456–6461. [CrossRef]
29. Ganesan, V.; Yoon, S. Hyper-Cross-Linked Porous Porphyrin Aluminum(III) Tetracarbonylcobaltate as a Highly Active Heterogeneous Bimetallic Catalyst for the Ring-Expansion Carbonylation of Epoxides. *ACS Appl. Mater. Interfaces* **2019**, *11*, 18609–18616. [CrossRef]
30. Padmanaban, S.; Gunasekar, G.H.; Lee, M.; Yoon, S. Recyclable Covalent Triazine Framework-based Ru Catalyst for Transfer Hydrogenation of Carbonyl Compounds in Water. *ACS Sustain. Chem. Eng.* **2019**, *7*, 8893–8899. [CrossRef]

31. Friend, C.M.; Xu, B. Heterogeneous Catalysis: A Central Science for a Sustainable Future. *Acc. Chem. Res.* **2017**, *50*, 517–521. [CrossRef]
32. Padmanaban, S.; Kim, M.; Yoon, S. Acid-mediated surface etching of a nano-sized metal-organic framework for improved reactivity in the fixation of CO_2 into polymers. *J. Ind. Eng. Chem.* **2019**, *71*, 336–344. [CrossRef]
33. von der Assen, N.; Bardow, A. Life cycle assessment of polyols for polyurethane production using CO_2 as feedstock: Insights from an industrial case study. *Green Chem.* **2014**, *16*, 3272–3280. [CrossRef]
34. Eberhardt, R.; Allmendinger, M.; Zintl, M.; Troll, C.; Luinstra, G.A.; Rieger, B. New zinc dicarboxylate catalysts for the CO_2/propylene oxide copolymerization reaction: Activity enhancement through Zn(II)-ethylsulfinate initiating groups. *Macromol. Chem. Phys.* **2004**, *205*, 42–47. [CrossRef]
35. Ree, M.; Hwang, Y.; Kim, J.S.; Kim, H.; Kim, G.; Kim, H. New findings in the catalytic activity of zinc glutarate and its application in the chemical fixation of CO_2 into polycarbonates and their derivatives. *Catal. Today* **2006**, *115*, 134–145. [CrossRef]
36. Wang, S.J.; Du, L.C.; Zhao, X.S.; Meng, Y.Z.; Tjong, S.C. Synthesis and characterization of alternating copolymer from carbon dioxide and propylene oxide. *J. Appl. Polym. Sci.* **2002**, *85*, 2327–2334. [CrossRef]
37. Zhong, X.; Dehghani, F. Solvent free synthesis of organometallic catalysts for the copolymerisation of carbon dioxide and propylene oxide. *Appl. Catal. B Environ.* **2010**, *98*, 101–111. [CrossRef]
38. Ang, R.R.; Sin, L.T.; Bee, S.T.; Tee, T.T.; Kadhum, A.A.H.; Rahmat, A.R.; Wasmi, B.A. Determination of zinc glutarate complexes synthesis factors affecting production of propylene carbonate from carbon dioxide and propylene oxide. *Chem. Eng. J.* **2017**, *327*, 120–127. [CrossRef]
39. Kim, J.S.; Kim, H.; Ree, M. Hydrothermal synthesis of single-crystalline zinc glutarate and its structural determination. *Chem. Mater.* **2004**, *16*, 2981–2983. [CrossRef]
40. Seth, S.; Matzger, A.J. Metal–Organic Frameworks: Examples, Counterexamples, and an Actionable Definition. *Cryst. Growth Des.* **2017**, *17*, 4043–4048. [CrossRef]
41. Miralda, C.M.; Macias, E.E.; Zhu, M.; Ratnasamy, P.; Carreon, M.A. Zeolitic Imidazole Framework-8 Catalysts in the Conversion of CO_2 to Chloropropene Carbonate. *ACS Catal.* **2012**, *2*, 180–183. [CrossRef]
42. Kim, J.; Kim, S.-N.; Jang, H.-G.; Seo, G.; Ahn, W.-S. CO_2 cycloaddition of styrene oxide over MOF catalysts. *Appl. Catal. A Gen.* **2013**, *453*, 175–180. [CrossRef]
43. Kumar, S.; Verma, G.; Gao, W.-Y.; Niu, Z.; Wojtas, L.; Ma, S. Anionic Metal–Organic Framework for Selective Dye Removal and CO_2 Fixation. *Eur. J. Inorg. Chem.* **2016**, *2016*, 4373–4377. [CrossRef]
44. Kuruppathparambil, R.R.; Babu, R.; Jeong, H.M.; Hwang, G.-Y.; Jeong, G.S.; Kim, M.-I.; Kim, D.-W.; Park, D.-W. A solid solution zeolitic imidazolate framework as a room temperature efficient catalyst for the chemical fixation of CO_2. *Green Chem.* **2016**, *18*, 6349–6356. [CrossRef]
45. Babu, R.; Kim, S.-H.; Kathalikkattil, A.C.; Kuruppathparambil, R.R.; Kim, D.W.; Cho, S.J.; Park, D.-W. Aqueous microwave-assisted synthesis of non-interpenetrated metal-organic framework for room temperature cycloaddition of CO_2 and epoxides. *Appl. Catal. A Gen.* **2017**, *544*, 126–136. [CrossRef]
46. Lin, Y.-F.; Huang, K.-W.; Ko, B.-T.; Lin, K.-Y.A. Bifunctional ZIF-78 heterogeneous catalyst with dual Lewis acidic and basic sites for carbon dioxide fixation via cyclic carbonate synthesis. *J. CO_2 Util.* **2017**, *22*, 178–183. [CrossRef]
47. Liang, J.; Huang, Y.-B.; Cao, R. Metal–organic frameworks and porous organic polymers for sustainable fixation of carbon dioxide into cyclic carbonates. *Coord. Chem. Rev.* **2019**, *378*, 32–65. [CrossRef]
48. Zhu, Q.; Meng, Y.Z.; Tjong, S.C.; Zhao, X.S.; Chen, Y.L. Thermally stable and high molecular weight poly(propylene carbonate)s from carbon dioxide and propylene oxide. *Polym. Int.* **2002**, *51*, 1079–1085. [CrossRef]
49. Kim, J.S.; Kim, H.; Yoon, J.; Heo, K.; Ree, M. Synthesis of zinc glutarates with various morphologies using an amphiphilic template and their catalytic activities in the copolymerization of carbon dioxide and propylene oxide. *J. Polym. Sci. Pol. Chem.* **2005**, *43*, 4079–4088. [CrossRef]
50. Wang, J.T.; Zhu, Q.; Lu, X.L.; Meng, Y.Z. ZnGA-MMT catalyzed the copolymerization of carbon dioxide with propylene oxide. *Eur. Polym. J.* **2005**, *41*, 1108–1114. [CrossRef]
51. Gao, L.J.; Luo, Y.C.; Lin, Y.J.; Su, T.; Su, R.P.; Feng, J.Y. Silica-supported zinc glutarate catalyst synthesized by rheological phase reaction used in the copolymerization of carbon dioxide and propylene oxide. *J. Polym. Res.* **2015**, *22*, 220. [CrossRef]

52. Klaus, S.; Lehenmeier, M.W.; Herdtweck, E.; Deglmann, P.; Ott, A.K.; Rieger, B. Mechanistic Insights into Heterogeneous Zinc Dicarboxylates and Theoretical Considerations for CO_2-Epoxide Copolymerization. *J. Am. Chem. Soc.* **2011**, *133*, 13151–13161. [CrossRef]
53. Sudakar, P.; Sivanesan, D.; Yoon, S. Copolymerization of Epichlorohydrin and CO_2 Using Zinc Glutarate: An Additional Application of ZnGA in Polycarbonate Synthesis. *Macromol. Rapid Commun.* **2016**, *37*, 788–793. [CrossRef] [PubMed]
54. Padmanaban, S.; Dharmalingam, S.; Yoon, S. A Zn-MOF-Catalyzed Terpolymerization of Propylene Oxide, CO_2, and β-butyrolactone. *Catalysts* **2018**, *8*, 393. [CrossRef]
55. Chisholm, M.H.; Navarro-Llobet, D.; Zhou, Z.P. Poly(propylene carbonate). 1. More about poly(propylene carbonate) formed from the copolymerization of propylene oxide and carbon dioxide employing a zinc glutarate catalyst. *Macromolecules* **2002**, *35*, 6494–6504. [CrossRef]
56. Kim, J.S.; Ree, M.; Shin, T.J.; Han, O.H.; Cho, S.J.; Hwang, Y.T.; Bae, J.Y.; Lee, J.M.; Ryoo, R.; Kim, H. X-ray absorption and NMR spectroscopic investigations of zinc glutarates prepared from various zinc sources and their catalytic activities in the copolymerization of carbon dioxide and propylene oxide. *J. Catal.* **2003**, *218*, 209–219. [CrossRef]
57. Rieter, W.J.; Taylor, K.M.L.; Lin, W. Surface Modification and Functionalization of Nanoscale Metal-Organic Frameworks for Controlled Release and Luminescence Sensing. *J. Am. Chem. Soc.* **2007**, *129*, 9852–9853. [CrossRef] [PubMed]
58. Cohen, S.M. Postsynthetic Methods for the Functionalization of Metal–Organic Frameworks. *Chem. Rev.* **2012**, *112*, 970–1000. [CrossRef] [PubMed]
59. Bhattacharya, B.; Haldar, R.; Dey, R.; Maji, T.K.; Ghoshal, D. Porous coordination polymers based on functionalized Schiff base linkers: Enhanced CO_2 uptake by pore surface modification. *Dalton Trans.* **2014**, *43*, 2272–2282. [CrossRef]
60. McGuire, C.V.; Forgan, R.S. The surface chemistry of metal–organic frameworks. *Chem. Commun.* **2015**, *51*, 5199–5217. [CrossRef]
61. Yin, Z.; Wan, S.; Yang, J.; Kurmoo, M.; Zeng, M.-H. Recent advances in post-synthetic modification of metal–organic frameworks: New types and tandem reactions. *Coord. Chem. Rev.* **2019**, *378*, 500–512. [CrossRef]
62. Ree, M.; Bae, J.Y.; Jung, J.H.; Shin, T.J. A new copolymerization process leading to poly(propylene carbonate) with a highly enhanced yield from carbon dioxide and propylene oxide. *J. Polym. Sci. Pol. Chem.* **1999**, *37*, 1863–1876. [CrossRef]
63. Ren, W.-M.; Liu, Z.-W.; Wen, Y.-Q.; Zhang, R.; Lu, X.-B. Mechanistic Aspects of the Copolymerization of CO_2 with Epoxides Using a Thermally Stable Single-Site Cobalt(III) Catalyst. *J. Am. Chem. Soc.* **2009**, *131*, 11509–11518. [CrossRef] [PubMed]